

01 Mar 1968

Interaction Potential between the Ground States of H and H⁻

Joseph C.Y. Chen

Jerry Peacher

Missouri University of Science and Technology, peacher@mst.edu

Follow this and additional works at: https://scholarsmine.mst.edu/phys_facwork

 Part of the [Physics Commons](#)

Recommended Citation

J. C. Chen and J. Peacher, "Interaction Potential between the Ground States of H and H⁻," *Physical Review*, vol. 167, no. 1, pp. 30-38, American Physical Society (APS), Mar 1968.

The definitive version is available at <https://doi.org/10.1103/PhysRev.167.30>

This Article - Journal is brought to you for free and open access by Scholars' Mine. It has been accepted for inclusion in Physics Faculty Research & Creative Works by an authorized administrator of Scholars' Mine. This work is protected by U. S. Copyright Law. Unauthorized use including reproduction for redistribution requires the permission of the copyright holder. For more information, please contact scholarsmine@mst.edu.

Interaction Potential between the Ground States of H and H⁻ †

JOSEPH C. Y. CHEN AND JERRY L. PEACHER

Department of Physics and Institute for Pure and Applied Physical Sciences, University of California, San Diego, La Jolla, California

(Received 14 July 1967)

An investigation of the interaction potential for H and H⁻ in both ungerade and gerade modes is carried out by a semiempirical method in which the recently observed isotope effect in dissociative attachment of electrons to hydrogen molecules is used. The interaction obtained is complex, and the imaginary parts of the interaction account for electron emissions during the course of the interaction. A comparison of the present result with other calculations is presented. The isotope effect in dissociative attachment is also discussed. It is shown that the ratios of the survival probabilities alone do not provide an adequate approximation for the isotope effect.

I. INTRODUCTION

IT is well known¹ that the Born-Oppenheimer (BO) separation approximation² provides a satisfactory description of molecular spectra as guided by the Franck-Condon principle.³ The adiabatic potential curves generated by the Born-Oppenheimer electronic states also provide, to an extent, a satisfactory approximation of the interaction potential of the corresponding atoms in collisions and reactions. Indeed, a class of chemical reactions can be qualitatively understood⁴ in terms of the adiabatic potential surface (or curves) obtained in the BO separation approximation.

Despite the success, there are, however, drawbacks in the adiabatic-potential-surface representation of the interaction potential for atomic collisions and reactions. This mainly arises from the fact that channel crossing and virtual excitation are not adequately taken into account in the adiabatic potential surface. Consequently, a large class of reactions such as recombinations, energy transfer, etc. cannot be satisfactorily interpreted in terms of the adiabatic potential curves.

One of the subtle difficulties of such an adiabatic Born-Oppenheimer representation lies in the noncrossing rule of von Neumann and Wigner⁵ which states that adiabatic BO potential curves of the same symmetry cannot cross. If one restricts oneself to the true adiabatic BO representation one then encounters the noncrossing dilemma (see Fig. 1). This difficulty has long been recognized in the early days of the development of molecular quantum theory. To overcome the noncrossing dilemma, the Landau-Zener theory, which provides a satisfactory description of slow reactive collisions by allowing pseudocrossing, has been developed.⁶ This

theory has been used with some qualitative success in interpreting atomic recombination processes in terms of multiple crossings.⁷ Recently the concept of curve crossing has been invoked to interpret^{8,9} the accurate measurements on electron-transfer processes in close encounters in the keV energy region.¹⁰ The quantities appearing in the Landau-Zener theory, however, depend critically on the choice of the pseudocrossing states, which are not precisely defined. This then results in considerable arbitrariness in the theory.

By decomposing the Feshbach projection operator for open channels¹¹ into channel projectors, an effective Hamiltonian for each open channel may be defined.¹² Utilizing such effective channel Hamiltonians, an alternative representation of the interaction potential for atomic collisions in the spirit of the Born-Oppenheimer separation approximation can be constructed. Such an interaction potential is basically energy-dependent, nonlocal, and complex, and is not constrained to the noncrossing rule. For the special case of atomic collisions with negative ions such as the (H,H⁻) system, it has been shown¹³ that the interaction potential so obtained corresponds to the resonant states appearing in the electron scattering by the residual H₂ molecule. Very encouraging results have already been achieved recently in utilizing such resonant states for interpreting reso-

Proc. Roy. Soc. (London) **A137**, 696 (1932); E. C. G. Stueckelberg, *Helv. Phys. Acta* **5**, 369 (1932).

⁷ J. L. Magee, *Discussions Faraday Soc.* **12**, 33 (1952); D. R. Bates and B. L. Moiseiwitsch, *Proc. Phys. Soc. (London)* **A67**, 805 (1954); D. R. Bates and J. T. Lewis, *ibid.* **A68**, 173 (1955).

⁸ W. Lichten, *Phys. Rev.* **131**, 229 (1961); **139**, A27 (1965); E. P. Ziemba and A. Russek, *ibid.* **115**, 922 (1959); R. P. Marchi and F. T. Smith, *ibid.* **139**, A1025 (1965).

⁹ The pseudocrossing states are referred to by Lichten as diabatic states (see Ref. 8).

¹⁰ See for example, G. J. Lockwood and E. Everhart, *Phys. Rev. Letters* **2**, 299 (1959); E. P. Ziemba and E. Everhart, *Phys. Rev. Letters* **2**, 299 (1959); V. V. Afrosimov, Yu. S. Gordeev, M. N. Panov, and N. V. Fedorenko, *Zh. Tekhn. Fiz.* **34**, 1613 (1964); **34**, 1624 (1964); **34**, 1637 (1964) [English transl.: *Soviet Phys.—Tech. Phys.* **9**, 1248 (1965); **9**, 1256 (1965); **9**, 1265 (1965)]; E. Everhart and Q. C. Kessel, *Phys. Rev. Letters* **14**, 247 (1965); D. C. Lorents and W. Aberth, *Phys. Rev.* **139**, A1017 (1965); **144**, 109 (1966).

¹¹ H. Feshbach, *Ann. Phys. (N. Y.)* **5**, 357 (1958); **19**, 287 (1962); L. Fonda and R. G. Newton, *ibid.* **10**, 490 (1960).

¹² J. C. Y. Chen, *Phys. Rev.* **152**, 1454 (1966).

¹³ J. C. Y. Chen, *Phys. Rev.* **156**, 12 (1967).

† This research was supported by the Advanced Research Projects Agency (Project DEFENDER) and was monitored by the U. S. Army Research Office (Durham) under Contract No. DA-31-124-ARO-D-257.

¹ G. Herzberg, *Spectrum of Diatomic Molecules* (D. Van Nostrand Co., Inc., New York, 1950).

² M. Born and J. R. Oppenheimer, *Ann. Physik* **84**, 457 (1927).

³ J. Franck, *Trans. Faraday Soc.* **21**, 536 (1925); E. U. Condon, *Phys. Rev.* **32**, 858 (1928).

⁴ S. Glasstone, K. J. Laidler, and H. Eyring, *The Theory of Rate Processes* (McGraw-Hill Book Co., Inc., New York, 1941).

⁵ J. von Neumann and E. P. Wigner, *Z. Physik* **30**, 467 (1929).

⁶ L. Landau, *Physik Z. Sowjetunion* **2**, 46 (1932); C. Zener,

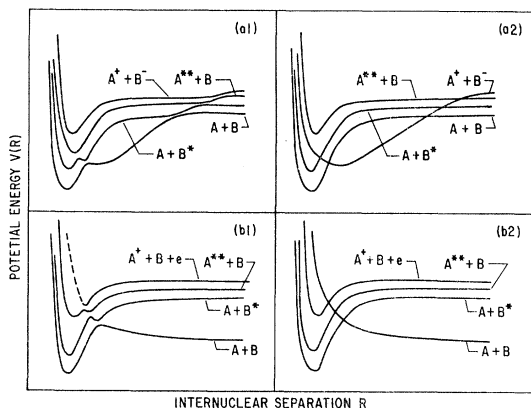


FIG. 1. Schematic diagrams of two sets of potential energies, a and b , of a typical molecule AB in two different representations, namely the adiabatic and pseudocrossing representations labeled by 1 and 2, respectively. Each set is formed by states of the same symmetry. In the adiabatic representation, the noncrossing rule prevents the ionic state and the dissociative state from crossing the remaining states in a and b sets, respectively, and gives rise to various dips and bumps as shown in (a1) and (b1). In the pseudocrossing representation, both the ionic state and the dissociative states are allowed to cross the remaining states as shown in (a2) and (b2), respectively. These crossings are of physical significance in ionic recombination, $A^+ + B^- \rightarrow A^{(*)} + B$, and in dissociative recombination, $e + AB^+ \rightarrow A^{(*)} + B$, processes.

nant vibrational and rotational excitation¹⁴ and dissociative attachment processes^{15,16} in electron scattering by molecules.

The purpose of the present communication is to demonstrate how such a potential can be obtained semiempirically for the (H, H^-) system when both H and H⁻ are in their ground states asymptotically. After a general discussion of the interaction potential between composite systems, the potential for H and H⁻ is then discussed in Sec. II. In Sec. III, we show that such an interaction potential for H and H⁻ can be obtained semiempirically from the measured isotope effects on the cross section for corresponding dissociative attachment. Our results are presented and discussed in Sec. IV where a comparison with other calculations is also made.

II. INTERACTION POTENTIAL BETWEEN H AND H⁻

The interaction potential between composite systems differs from the usual adiabatic potential curves in two major respects, namely, the virtual-excitation and multichannel effects. Virtual excitation into the closed channel segment gives rise to a nonlocal effect which is in general energy-dependent and becomes more appreciable with increasing collision energy for most systems.

¹⁴ J. C. Y. Chen, *Phys. Rev.* **146**, 61 (1966); *J. Chem. Phys.* **45**, 2710 (1966); **40**, 3513 (1964); A. Herzenberg and F. Mandl, *Proc. Roy. Soc. (London)* **A270**, 48 (1962); J. C. Y. Chen and J. L. Magee, *J. Chem. Phys.* **36**, 1407 (1962).

¹⁵ J. C. Y. Chen, *Phys. Rev.* **148**, 66 (1966); T. F. O'Malley, *ibid.* **150**, 14 (1966); **155**, 59 (1967).

¹⁶ J. N. Bardsley, A. Herzenberg, and F. Mandl, *Proc. Phys. Soc. (London)* **89**, 321 (1966).

The multichannel effects which result from the partitioning of the collision amplitude into various channels can be accounted for by using a complex potential. The imaginary parts of the interaction potential then account for the absorption or emission in the channel amplitude. Thus the appropriate potential for interacting composite systems such as H and H⁻ is in general energy-dependent, nonlocal, and complex.

For low-energy (thermal-room-temperature) collisions, the nonlocal effect of the potential becomes unimportant for the (H, H^-) system if we confine our interest to cases where both H and H⁻ are in their ground states asymptotically. This is possible because the corresponding molecular states are widely separated due to the strong local electric field along the internuclear axis. The multichannel effect, however, is of importance even for very low-energy collisions between H and H⁻. This is because both the scattering channel $H + H^- \rightarrow H + H^-$ and the electron-transfer channel $H + H^- \rightarrow H^- + H$ are strongly coupled with the exothermic associative-detachment channel $H + H^- \rightarrow H_2 + e$.^{13,17} In addition, at somewhat higher energies, the coupling with the collisional-detachment channel $H + H^- \rightarrow H + H + e$ is also of importance. To account for this coupling of the associative- and collisional-detachment channels, the interaction potential is made complex. Thus, the imaginary parts of the potential account for electron emission into the associative- and collisional-detachment channels. Since there is no threshold for the associative-detachment process, the imaginary parts of the interaction are effective even at zero-energy collisions between H and H⁻.

The physical picture is as follows. The interaction potential for H and H⁻ at small internuclear separation splits, due to the local electric field created along the internuclear axis, into the gerade and ungerade modes, corresponding to the $^2\Sigma_g^+$ and $^2\Sigma_u^+$ H_2^- states, respectively. Each of these states is related to the compound states which arise in the electron scattering by the residual H_2 molecule. In considering the interaction potential between H and H⁻ in their ground states, we are here dealing with both of the states. The two H_2^- states cross the potential curve of the H_2 molecule in the $^1\Sigma_g^+$ state with a continuum electron. Thus when H and H⁻ come closer than the crossing internuclear separation in the ungerade (or gerade) mode, the interaction potential becomes complex due to the coupling with the associative-detachment channel. In addition, the gerade mode of interaction may also cross the potential curve of the H_2 molecule in the $^3\Sigma_u^+$ state with a continuum electron. This permits electron emission into the collisional-detachment channel via the $^3\Sigma_u^+$ state of H_2 (see Fig. 8).

Here we actually encounter potential crossing of H_2^-

¹⁷ J. C. Y. Chen, in *Proceedings of the Fifth International Conference on the Physics of Electronic and Atomic Collisions* (Publishing House Nauka, Leningrad, USSR, 1967), p. 332.

and H_2+e , i.e., crossing of a bound electronic state to a continuum electronic state. The differences in symmetry between H_2^- and H_2 can be made up by the free electron so that H_2+e considered as a whole has the same symmetry as H_2^- . Thus in the true BO adiabatic sense, the curves of bound H_2^- states coming from the right will touch but not cross the H_2 curve. The curves coming from the left correspond to the compound H_2^- states and may cross the H_2 curve but will *not necessarily* join smoothly onto the potential curves of the bound H_2^- state. This is clear since the S -matrix pole associated with the compound H_2^- state lies in the unphysical sheet and is in general not the same S -matrix pole associated with the bound H_2^- state in the physical sheet. In the present semiempirical study we will assume, however, that the phenomenological potential curves are smooth in the neighborhood of the crossing.

Calculation of the interaction potential for both the ${}^2\Sigma_u^+$ and ${}^2\Sigma_g^+$ configurations of H_2^- have been carried out using a conventional Rayleigh-Ritz variation method.¹⁸ It was pointed out¹⁹ that for such states there is no minimum principle which guarantees upper bounds since these states cross the $H_2({}^1\Sigma_g^+)+e$ state and are imbedded in the continuum. In view of the fact that the H_2^- states are auto-ionizing and not stationary states, an alternative method, adopted from Feshbach's theory,¹¹ was suggested by one of the authors^{20,21} to calculate such states. In this method, one projects out from the full Hilbert space of the total Hamiltonian the ground ${}^1\Sigma_g^+$ H_2 residual molecular state and thereby eliminates the coupling with the continuum associated with the ${}^1\Sigma_g^+$ H_2 residue state. The quasistationary representation of the H_2^- states can then be obtained from the remaining diagonal Hamiltonian QHQ , where $Q=1-P$ and P is the projection operator which projects onto the ${}^1\Sigma_g^+$ H_2 residue state. From these quasistationary states, both the real and imaginary parts of the interaction potential (including the shift in interaction energy due to the off-diagonal Hamiltonian PHQ) can then be in principle calculated. It should be noted that the minimum principle for the QHQ Hamiltonian holds only if a complete decoupling of the true residual molecular state including exchange effects can be achieved.²² A calculation in accordance with this

general idea was later carried out²³ for the real part of the interaction potential of H_2^- . It is not clear from the calculation whether a complete decoupling of the residual molecular states with exchange effects has been appropriately carried out.

The Feshbach-type description of an auto-ionization (resonant or compound) state is appropriate for cases where the active electron is bound to an excited field generated by some excited residual molecular states. This provides an adequate description for the ${}^2\Sigma_g^+$ H_2^- resonant state, since the dominant excited H_2 state can be identified as the ${}^3\Sigma_u^+$ state. For the ${}^2\Sigma_u^+$ H_2^- auto-ionization state, the Feshbach description is not appropriate without modification,²⁴ since here the incident electron is in resonance with the ground ${}^1\Sigma_g^+$ H_2 state. Ordinarily one would not expect a static field generated by a ground target state to be capable of supporting a temporary bound state. In the ${}^2\Sigma_u^+$ case, the extra strength comes from the centrifugal barriers associated with various odd partial waves of the active electron. We have recently shown²⁵ that the ${}^2\Sigma_u^+$ H_2^- state is actually a low-lying p -wave resonance in slow electron scattering by hydrogen molecules. This then requires a modification of the Feshbach prescription for calculating the ${}^2\Sigma_u^+$ auto-ionization state.²⁴

Independently, Bardsley *et al.* have suggested²⁶ that such auto-ionization states may be interpreted as Kapur-Peierls resonant states. A stationary expression was derived for the calculation of both the real and imaginary parts of the interaction potential. An *a priori* calculation of the interaction for H and H^- both in the ungerade and gerade modes has been carried out recently.²⁷ This set of calculated potentials does not, however, give quantitative agreement with various measurements unless an arbitrary scaling parameter is used.^{16,25} This is not surprising in view of the cutoff radius used for the electron-molecule interaction²⁸ and the crude trial wave function used in the calculation. We show in the next section that by utilizing the measured isotope

²³ H. S. Taylor and J. K. Williams, *J. Chem. Phys.* **42**, 4063 (1965).

²⁴ This modification can be carried out in terms of channel projectors. For this particular case, one simply solves the set of coupled equations projected onto the scattering, $H+H^- \rightarrow H+H^-$, and associative-detachment, $H+H^- \rightarrow H_2+e$, channels in the open-channel segment of the Hilbert space as shown in Ref. 13 (in particular Sec. IV.1). For further details, see Ref. 17.

²⁵ J. C. Y. Chen and J. L. Peacher, *Phys. Rev.* **163**, 103 (1967).

²⁶ J. N. Bardsley, A. Herzenberg, and F. Mandl, in *Atomic Collision Processes*, edited by M. R. C. McDowell (North-Holland Publishing Company, Amsterdam, 1964), p. 415.

²⁷ J. N. Bardsley, A. Herzenberg, and F. Mandl, *Proc. Phys. Soc. (London)* **89**, 305 (1966).

²⁸ Since the electromagnetic interaction present in the molecular system is of a long-range nature, the treatment of resonant states with a joining radius outside of which the interaction of the electron with the molecule is neglected is not accurate. One possible improvement of the treatment is to treat interaction outside of the joining radius as a perturbation. Here the difficulty lies in preserving the Kapur-Peierls-type boundary condition so that scattering at the joining radius is appropriately taken into account. One of the authors (J.C.Y.C.) is grateful to Professor R. E. Peierls for helpful discussions on the applicability of the Kapur-Peierls resonance theory to molecular systems.

¹⁸ H. Eyring, J. O. Hirschfelder, and H. S. Taylor, *J. Chem. Phys.* **4**, 439 (1936); A. Dalgarno and H. R. C. McDowell, *Proc. Phys. Soc. (London)* **A69**, 615 (1956); B. K. Gupta, *Physica* **35**, 190 (1959); **26**, 335 (1960); I. Fircher-Hjalmsous, *Arkiv Fysik* **16**, 33 (1959).

¹⁹ J. C. Y. Chen, thesis, University of Notre Dame, 1961 (unpublished); E. R. Davidson, *J. Chem. Phys.* **36**, 1080 (1962); H. S. Taylor and F. E. Harris, *ibid.* **39**, 1012 (1963).

²⁰ J. C. Y. Chen, *J. Chem. Phys.* **40**, 3507 (1964), see in particular Sec. III and Eq. (3.2); in *Atomic Collision Processes*, edited by M. R. C. McDowell (North-Holland Publishing Company, Amsterdam, 1964), p. 428.

²¹ The projection operator technique has recently been applied to both associative detachment and dissociative attachment processes; see Refs. 13 and 15.

²² Y. Hahn, T. F. O'Malley, and L. Spruch, *Phys. Rev.* **128**, 932 (1962).

effects on the cross section for dissociative attachment a semiempirical improvement of the complete complex interaction potential is possible.

III. SEMIEMPIRICAL PROCEDURE

The process of dissociative attachment for the (*e*,H₂) system may proceed via either the ²Σ_u⁺ or ²Σ_g⁺ quasi-stationary states of H₂⁻ at appropriate incident electron energies.^{15,16,29} Since these two states are far apart, the energy regions where the cross section become appreciable do not overlap. We may therefore treat the two modes of dissociative attachment independently of each other. For given initial vibrational and rotational states, *v* and *L*, of the H₂ target molecule in the ground ¹Σ_g⁺ state, the cross section for the two modes of dissociative attachment is given, to a reasonable approximation, by²⁵

$$\sigma_{vL}^{(u)} = (\kappa/k_i)\beta_1^{(u)}(R_e)G_{vL}(g \rightarrow u), \quad (3.1)$$

$$\sigma_{vL}^{(g)} = (\kappa/k_i)\beta_0^{(g)}(R_e)G_{vL}(g \rightarrow g), \quad (3.2)$$

with

$$G_{vL}(g \rightarrow u) = \mu C_{L+1} |\langle \xi_{L+1}^{(u)} | \chi_v \rangle|^2 P_{L+1}^{(u)} + \mu C_{L-1} |\langle \xi_{L-1}^{(u)} | \chi_v \rangle|^2 P_{L-1}^{(u)}, \quad (3.3)$$

$$G_{vL}(g \rightarrow g) = \mu |\langle \xi_L^{(g)} | \chi_v \rangle|^2 P_L^{(g)}, \quad (3.4)$$

where *k_i* and *κ* are the wave numbers of the incident electron and relative motion of H and H⁻, respectively, *β₁*^(*u*) and *β₀*^(*g*) are the absolute square of the electronic matrix elements in the ungerade and gerade modes, respectively, evaluated at the equilibrium internuclear separation *R_e* of the ground hydrogen target states, *χ_v* is the initial vibrational wave function, *ξ_L*^(*u*) and *ξ_L*^(*g*) are the continuum radial nuclear wave functions in the ungerade and gerade modes, respectively, *μ* is the reduced mass of the molecule, the *C_L*'s are related to the

Clebsch-Gordan coefficients, and the *P_L*'s are the survival probabilities against electron decay. The continuum radial nuclear wave functions are solutions of a pair of Schrödinger equations with complex potentials

$$\{d^2/dR^2 - J(J+1)/R^2 + 2\mu[E - V_u(R) + \frac{1}{2}i\Gamma_u(R)]\} \times \xi_J^{(u)}(R) = 0, \quad (3.5a)$$

$$\{d^2/dR^2 - J(J+1)/R^2 + 2\mu[E - V_g(R) + \frac{1}{2}i\Gamma_g(R)]\} \times \xi_J^{(g)}(R) = 0, \quad (3.5b)$$

where *V_u* - $\frac{1}{2}i\Gamma_u$ and *V_g* - $\frac{1}{2}i\Gamma_g$ are the complex potentials for the ungerade and gerade modes of interaction. Equations (3.6) are solved with the boundary conditions

$$\xi_J^{(u,g)}(R) \xrightarrow{R \rightarrow \infty} \kappa^{-1} \sin(\kappa R - \frac{1}{2}J\pi + \eta_J^{(u,g)}), \quad (3.6)$$

where

$$\eta_J^{(u,g)} = \delta_J^{(u,g)} + i\zeta_J^{(u,g)}. \quad (3.7)$$

The survival probabilities are energy-dependent and are expressed in terms of the corresponding imaginary parts of the radial phase shifts *η_L*^(*u,g*) [Eq. (3.7)]:

$$P_L^{(u,g)} = \exp\{-2\zeta_L^{(u,g)}\}. \quad (3.8)$$

In writing down Eqs. (3.1)–(3.4), we have made explicit use of the Kronig selection rules and the parity symmetries of the system, and have kept only the lowest contributing partial waves of the incident electron.²⁵

Examining Eqs. (3.1) and (3.2), it is apparent that since the *β*'s are very weakly mass-dependent and can, for most practical purposes, be considered mass-independent, the ratios of the cross section for different isotopes of the target hydrogen molecule are independent of the electronic matrix elements. We then have for H₂ and HD, for example,

$$\frac{\bar{\sigma}^{(u,g)}(E, T, \text{H}_2)}{\bar{\sigma}^{(u,g)}(E, T, \text{HD})} = \left(\frac{Z(\text{HD})}{Z(\text{H}_2)} \right) \frac{\sum_v \sum_L' (2L+1) \kappa(\text{H}_2) G_{vL}^{\text{H}_2}(g \rightarrow u, g) e^{-[\epsilon_v(\text{H}_2) + \epsilon_L(\text{H}_2)]/KT}}{\sum_{v'} \sum_{L'}' (2L'+1) \kappa(\text{HD}) G_{v'L'}^{\text{HD}}(g \rightarrow u, g) e^{-[\epsilon_{v'}(\text{HD}) + \epsilon_{L'}(\text{HD})]/KT}}, \quad (3.9)$$

where *Z*⁻¹ is the partition function of the target molecule. In anticipating, to compare with the experimental results, we have carried out in Eq. (3.9) a thermal average of the cross section over the distribution of the initial vibrational and rotational states of the target molecule,

$$\bar{\sigma}^{(u,g)}(E, T) = \frac{\beta_{1,0}^{(u,g)}}{Z} k_i \times \sum_v \sum_L' 2(2L+1) \kappa G_{vL}(g \rightarrow u, g) e^{-[\epsilon_v + \epsilon_L]/KT}, \quad (3.10)$$

where the prime on the sum over *L* indicates a restriction in the *L* sum imposed by the symmetry requirement of the total target molecular wave function in interchanging the constituent nuclei when they are identical. Thus, in the case of H₂ we have, for example,

$$\sum_L' = \sum_{\text{even } L} + 3 \sum_{\text{odd } L}. \quad (3.11)$$

The lower limits in sums over *v* and *L* are restricted by the threshold energy. We are interested in experimental measurements which are carried out at room temperature so that excited electronic states need not be included in the averaged sum.

Now if the interaction potential for H and H⁻ is known, both the radial wave functions *ξ_L*^(*u,g*) and the

²⁹ (a) For the ungerade case, G. J. Schulz and R. K. Asundi, Phys. Rev. **158**, 25 (1967); Phys. Rev. Letters **15**, 946 (1965). (b) For the gerade case, D. Rapp, T. E. Sharp, and D. D. Briglia, Phys. Rev. Letters **14**, 533 (1965).

imaginary parts of the radial phase shift $\zeta_L^{(u,\theta)}$ can be calculated in a straightforward manner so that the G functions are uniquely determined. The isotope effect can therefore be predicted. It was suggested by Demkov³⁰ that the observed isotope effect in dissociative attachment can be explained by the mass dependence of the survival probability alone. This, however, is not a good approximation in general since the mass dependence of the nuclear overlap integrals cannot be treated as a constant. One can easily see that the similarity transformation by mass scaling in the nuclear integral does not factor out the mass dependence completely. Consequently the continuum nuclear wave function has an inherent mass dependence which can be enhanced by a large imaginary component of the complex potential.

To demonstrate this observation, it is sufficient to examine the coefficients in the asymptotic expression [Eq. (3.6)] for the continuum nuclear wave function. Since the phase shifts $\eta_J^{(u,\theta)}$ are complex, Eq. (3.6) can, with the help of Eq. (3.7), be rewritten as

$$\begin{aligned} \xi_J^{(u,\theta)}(R) &\xrightarrow{R \rightarrow \infty} (e^{iJ} / 2\kappa) \\ &\times \left\{ (1 + P_J^{(u,\theta)}) \sin(\kappa R - \frac{1}{2}J\pi + \delta_J^{(u,\theta)}) \right. \\ &\left. + i(1 - P_J^{(u,\theta)}) \cos(\kappa R - \frac{1}{2}J\pi + \delta_J^{(u,\theta)}) \right\}. \end{aligned} \quad (3.12)$$

This demonstrates that the mass dependence of $\xi_J^{(u,\theta)}(R)$ arising from the imaginary parts of the phase shifts is comparable to the survival probability itself. The mass dependence arising from the real parts of the phase shifts is very weak since $\delta_J^{(u,\theta)}$ appears in the argument of rapidly varying trigonometric functions. Now if the imaginary parts of the interaction are switched off (i.e., to take $\zeta_J^{(u,\theta)}$ to be zero), Eq. (3.12) reduces to a simple sine function and the mass dependence of $\xi_J^{(u,\theta)}(R)$ becomes very weak. In this case the survival probability becomes unity and is not mass-dependent. This observation of the mass dependence of the nuclear overlap integral is also verified by detailed numerical calculations presented in Sec. IV.

It should be noted that from the isotope effects given by Eq. (3.9), the interaction potential cannot, however, be deduced uniquely, since there is a set of complex potentials which would yield the same isotope effect. This arbitrariness can, nevertheless, be considerably removed if we demand that the deduced potential would yield the correct isotope effect not only for several isotopes but also for the entire energy region where the cross section is appreciable. Note that here we are seeking for a complex but local potential. Since the classical turning point R_0 of the interaction potential changes with energy, the survival probabilities and nuclear overlap integrals will then change accordingly so that a different isotope effect results. By requiring the fit to extend over the significant energy region, we

are in effect tracing the trajectory of the classical turning point of the interaction potential as a function of energy. The topology of the interaction energy can then be adequately mapped at least within the Franck-Condon region of the target molecule. Utilizing further the knowledge of the atomic states at large internuclear separation, an interaction potential over significant internuclear separations can then be approximately determined.

To determine the interaction potential from ratios of isotope cross sections, functional forms for both the real and imaginary parts of the potential must first be chosen explicitly. We adopted for the ungerade mode of interaction the forms

$$V_u(R) = D_e^{(u)} \{ e^{-2\alpha_u(R-R_e^{(u)})} - 2e^{-\alpha_u(R-R_e^{(u)})} \}, \quad (3.13a)$$

$$\Gamma_u(R) = \gamma_u e^{-\lambda_u(R-\delta_u)^2}, \quad (3.13b)$$

and for the gerade mode of interaction

$$V_g(R) = \mu_g e^{-\alpha_g R}, \quad (3.14a)$$

$$\Gamma_g(R) = \gamma_g e^{-\lambda_g(R-\delta_g)^2}. \quad (3.14b)$$

These choices were made primarily because they fit well to the shape of the H_2^- potential curves calculated recently by Bardsley *et al.*²⁷ The two sets of parameters $\{D_e^{(u)}, \alpha_u, R_e^{(u)}, \gamma_u, \lambda_u, \delta_u\}$ and $\{\mu_g, \alpha_g, \gamma_g, \lambda_g, \delta_g\}$ so determined serve as our starting values for searching until the isotope effect predicted by Eq. (3.6) reproduces reasonably well that which is observed experimentally over the entire energy region where the cross section is appreciable. Detailed measurements of the isotope effect for dissociative attachment have been recently made for both ungerade and gerade cases.²⁹ This makes the semiempirical determination of the potential possible.

As discussed before that the gerade mode of interaction may cross the $^3\Sigma_u^+$ state of H_2 at a certain internuclear separation R_c . This then results in electron emission into the $^3\Sigma_u^+$ state of H_2 for $R < R_c$. If the results for the generalized analyticity and unitarity of the S matrix³¹ holds for the (e, H_2) multichannel system for each given internuclear separation of the H_2 molecules, some typical behavior of the path of the $^2\Sigma_g^+$ state on the complex energy plane is expected in the neighborhood of the crossing.

For $R > R_c$, the pole in the s matrix associated with the $^2\Sigma_g^+ H_2^-$ state lies on an unphysical sheet which can be reached from the physical sheet by crossing the branch cut corresponding to the $^1\Sigma_g^+$ elastic threshold. This unphysical sheet is called sheet 2. For $R < R_c$ the $^2\Sigma_g^+ H_2^-$ state lies above the $^3\Sigma_u^+$ inelastic threshold and the corresponding pole may lie on any of the two new unphysical sheets created by the opening of the $^3\Sigma_u^+$ inelastic threshold. One of the sheets is far removed from the physical sheet and is not physically significant. The other sheet (sheet 3) is physically significant and

³⁰ Yu. N. Demkov, Phys. Rev. Letters **15**, 235 (1965).

³¹ R. J. Eden and J. R. Taylor, Phys. Rev. **133**, B1575 (1964).

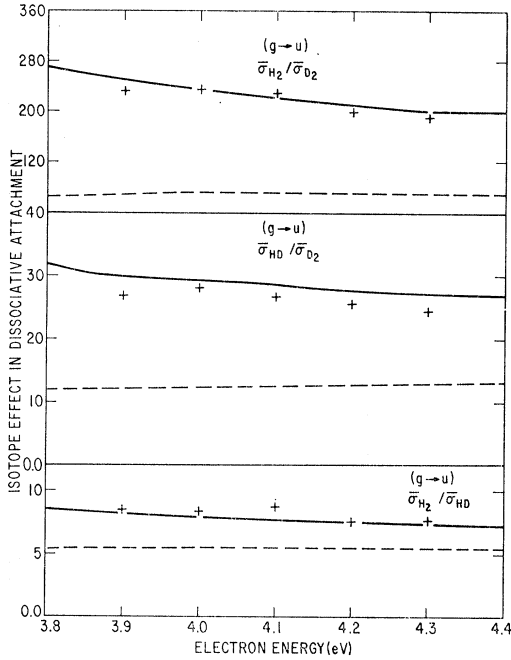


FIG. 2. Comparison of the isotope effect in the $g \rightarrow u$ dissociative attachment predicted by the interaction potential [Eq. (4.1)] (solid curves) with the experimental observations (crosses) of Schulz and Asundi in Ref. 29(a). The dashed curves are the isotope effect predicted by the interaction potential calculated by Bardsley *et al.* in Ref. 27.

can be reached from the physical sheet by crossing two branch cuts corresponding to the elastic and inelastic thresholds. Now if there is only a single pole associated with the ${}^2\Sigma_g^+$ state, one encounters an interesting situation in which the pole for the ${}^2\Sigma_g^+$ state lies on one sheet, namely sheet 2, for $R > R_c$ and on a different sheet, namely sheet 3, for $R < R_c$. In order for the pole to reach sheet 3 from sheet 2, it must loop around the ${}^3\Sigma_u^+$ inelastic branch point. As a consequence the scattering amplitude must have a dip at the crossing and the imaginary energy Γ_g must have a sharp dip near the crossing.³² There is also the possibility that more than one pole is associated with the ${}^2\Sigma_g^+$ H₂⁻ state. In this case the poles need not change Riemann sheets.

Now if indeed only a single pole is associated with the ${}^2\Sigma_g^+$ state and lies on sheet 3 for $R < R_c$, the expression Eq. (3.14b) adopted for Γ_g should then be modified to account for the expected dip. Without accurate information on the interaction potential for the projectile electron, the detailed manner of going through the dip is, however, not clear. This makes the semiempirical parametrization method very difficult. To test if the semiempirical procedure adopted here is sufficiently sensitive to the dip, we investigated the case where the dip is approximated by a square well. We found, how-

³² This behavior was first pointed out by P. G. Burke (private communication). One of the authors (J.C.Y.C.) is grateful to Professor P. G. Burke and Professor David Wong for helpful discussions concerning this behavior.

ever, that the phenomenological potential obtained by the semiempirical method is not very sensitive to the dip in Γ_g provided the area of the dip is not large. Thus the smooth-type curve given by Eq. (3.14b) constitutes a reasonable approximation for Γ_g .

IV. RESULTS AND DISCUSSION

Utilizing the semiempirical procedures proposed in Sec. III, a set of interaction potentials which simulate reasonably well the observed isotope effect over the significant energy regions is found. They are given by

$$V_u(R) = 0.5 \{ \exp[-1.7773(R-2.33)] - 2 \exp[-0.88865(R-2.33)] \}, \quad (4.1a)$$

$$\Gamma_u(R) = 3.08 e^{-0.386(R-0.9)^2}, \quad (4.1b)$$

$$V_g(R) = 57 e^{-1.4886R}, \quad (4.2a)$$

$$\Gamma_g(R) = 1.16 e^{-0.28(R-1.2)^2}, \quad (4.2b)$$

where both the V 's and Γ 's are in units of electron volts and R is in units of the Bohr radius a_0 . A comparison of the predicted isotope effect with experimental observation²⁹ using the above potentials is given in Figs. 2 and 3 for the ungerade and gerade cases, respectively. The agreement is slightly better for the gerade case than it is for the ungerade case. This is probably due to the fact that for the ungerade case the measurement is more difficult because of the low intensity. In matching the theoretical results with the experimental results, we folded into the theoretical cross sections the electron distribution which characterizes the electron beam used in the experiments.

The isotope effect presented in Figs. 2 and 3 is calculated from Eq. (3.9) and not from the ratios of the survival probability. As discussed in Sec. III, the nuclear overlap integral which appears in the G functions [Eqs. (3.3) and (3.4)] can be strongly mass-dependent, which results from the imaginary parts of the interaction [see Eq. (3.12)]. In Figs. 4 and 5 the absolute squares of the overlap integrals for different hydrogen isotopes are plotted for the $g \rightarrow u$ and $g \rightarrow g$

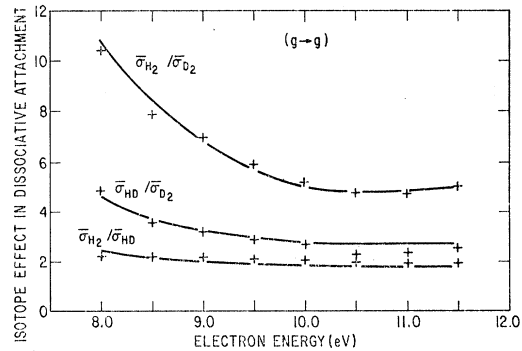


FIG. 3. Comparison of the isotope effect in the $g \rightarrow g$ dissociative attachment predicted by the interaction potential [Eq. (4.2)] (solid curves) with the experimental observation (crosses) of Rapp, Sharp, and Briglia in Ref. 29(b).

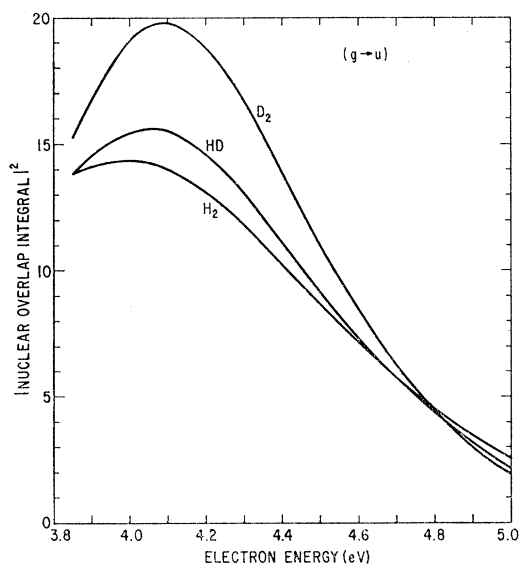


FIG. 4. Isotope effect in the absolute square of the nuclear overlap integral between a bound and a continuum state for the $g \rightarrow u$ dissociative attachment in the (e, H_2) system.

dissociative attachments, respectively. It is seen from these figures that the mass dependence of the overlap integral in these two cases are actually reversed in order. For the $g \rightarrow g$ case where the corresponding imaginary part of the interaction is relatively smaller, the mass dependence follows the $\mu^{-5/8}$ behavior for the regular nuclear overlap integrals between the bound and continuum states³³ for most incident electron energies. For the $g \rightarrow u$ case the mass dependence is reversed from the $\mu^{-5/8}$ behavior due to the large imaginary interaction. This clearly demonstrates that the isotope effect in dissociative attachment is not adequately approximated by the ratios of the survival probabilities alone. An interesting isotope effect for dissociative attachment has recently been observed in methane³⁴ and water.³⁵

The interaction potentials given by Eqs. (4.1) and (4.2) are plotted in Figs. 6 and 7. For comparison, the interaction potentials obtained by Bardsley *et al.*²⁷ are also included in Figs. 6 and 7. It is seen from Fig. 6 that the agreement between the two calculations is reasonably good for the real part of the $^2\Sigma_u^+$ interaction potential. However, for the $^2\Sigma_g^+$ interaction and the imaginary part of the $^2\Sigma_u^+$ interaction the agreement is rather poor. The maximum Γ obtained in the present treatment is in general smaller than that obtained by

³³ It should be noted that sometimes the μ factor in Eqs. (3.3) and (3.4) is defined to be included in the nuclear overlap integral. In this case, the approximate mass dependence for the regular nuclear overlap integral between the bound and continuum nuclear states should be $\mu^{-1/8}$. In both cases the mass dependence of the "capture cross" is $\mu^{1/4}$. This mass dependence does not constitute however, a reliable approximation for cases where the interaction potential is complex.

³⁴ T. E. Sharp and J. T. Dowell, *J. Chem. Phys.* **46**, 1530 (1967).
³⁵ R. N. Compton and L. G. Christophorou, *Phys. Rev.* **154**, 110 (1967).

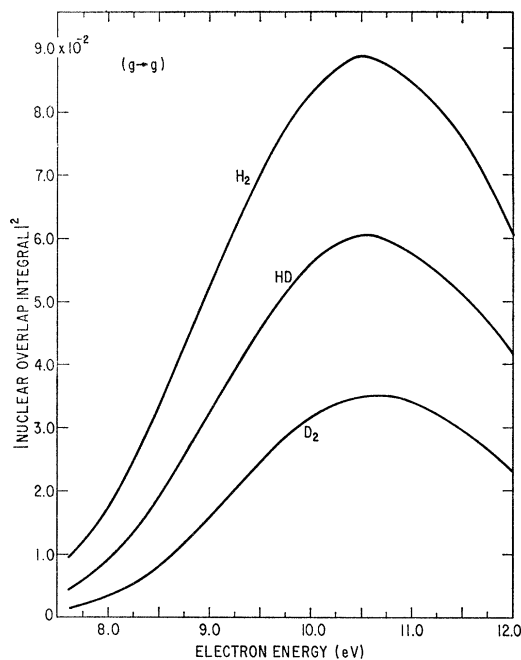


FIG. 5. Isotope in the absolute square of the nuclear overlap integral between a bound and a continuum state for the $g \rightarrow g$ dissociative attachment in the (e, H_2) system.

Bardsley *et al.* as shown in Fig. 7. Calculation of the isotope effects using Eq. (3.9) has also been carried out for the set of potentials obtained by Bardsley *et al.* and is plotted in Fig. 2 as dashed curves for the $g \rightarrow u$ dissociative attachment. It is seen that the isotope effect for the $g \rightarrow u$ case is underestimated by their potential.

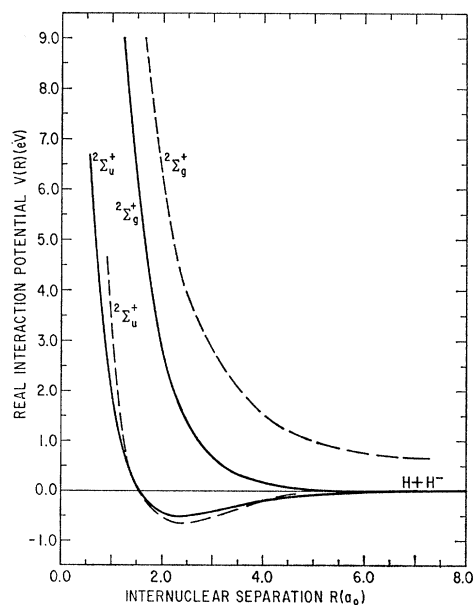


FIG. 6. Comparison of the real parts of the interaction potential between the ground states of H and H^- obtained in the present treatment (solid curves) with those obtained by Bardsley *et al.* (dashed curves) in Ref. 27.

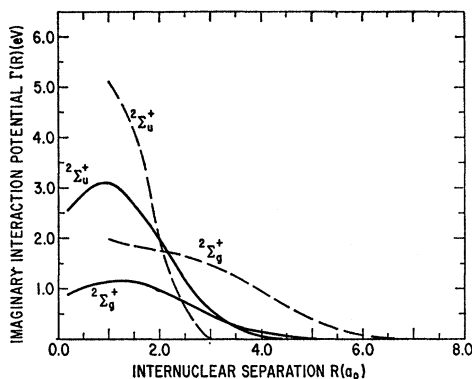


FIG. 7. Comparison of the imaginary parts of the interaction potential between the ground states of H and H⁻ obtained in the present treatment (solid curves) with those obtained by Bardsley *et al.* (dashed curves) in Ref. 27.

For the $g \rightarrow g$ case, their potential overestimates the isotope effect by two orders of magnitude, so their results are not included in Fig. 3. The fair agreement for the isotope effect in the $g \rightarrow g$ case was obtained by Bardsley *et al.*¹⁶ only after introducing a scaling parameter which reduces by approximately 50% the exponent in the survival probability.

In Fig. 8 the real parts of the interaction potential are plotted together with the potential curves of the parent H₂ molecule³⁶ with a continuum electron. It is seen from this figure that the ungerade and gerade modes of interaction for H and H⁻ cross the $^1\Sigma_g^+$ state of H₂ at $R=3.35a_0$ and $3.85a_0$, respectively. Examining Fig. 7 one observes that the imaginary parts of the two modes of interaction first become appreciable at internuclear separations corresponding closely to the respective crossing points in Fig. 8. This is consistent with the theoretical picture that electron emission occurs after the colliding partners H and H⁻ approach each other to distances which are comparable with or smaller than the crossing distances. It is also observed in Fig. 8 that the $^2\Sigma_g^+$ gerade mode of interaction also crosses the $^3\Sigma_u^+$ state of H₂ at an internuclear separation lying within the Franck-Condon region of the $^1\Sigma_g^+$ state of the H₂ molecule. This suggests that at regions where the electron emission amplitude to the associative-detachment channel would be normally large according to the Franck-Condon principle, the competitive collisional-detachment channel becomes significant. One must then consider the partition of the electron emission amplitude into the $H+H^- \rightarrow H+H+e$ collisional detachment channel. This could give rise to the slight dip observed in the $g \rightarrow g$ dissociative attachment.^{29b,37}

It is worthwhile to mention that a Morse-type potential usually gives rise to a repulsive potential which is too soft to be realistic for most molecular systems at small R . In our fitting to the ungerade mode of interaction, perhaps a different functional form which

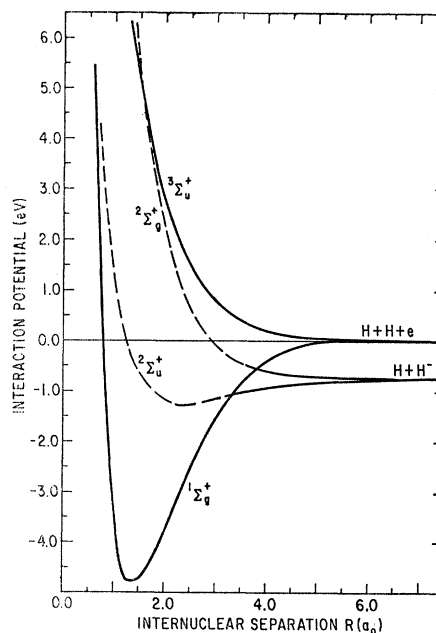


FIG. 8. The relation of the interaction potential between H and H⁻ in their ground states with the residual H₂ molecules in the $^1\Sigma_g^+$ and $^3\Sigma_u^+$ states in the presence of a continuum electron.

makes the repulsive part of the interaction stronger should be used. We found that inaccuracy introduced by the softness of the repulsive portion of the potential is relatively small in comparison with the inaccuracy involved in the fitting procedure. Such an improvement does not seem warranted in view of the present status of the quantitative nature of the theoretical and experimental results. The accuracy of the interaction potential deduced in the present treatment is bounded among other things by the experimental accuracy. Application of the interaction potential has recently been carried out with encouraging results for resonant electron transfer¹⁷ and for associative detachment³⁸ in the (H,H⁻) collision system.

Note added in manuscript. We note that by mapping the isotope effect in dissociative attachment over the incident electron energy regions where the cross section is appreciable we are in fact tracing the classical turning points for the $^2\Sigma_u^+$ and $^2\Sigma_g^+$ states of H₂⁻, lying above the threshold for dissociative attachment. This allows us to obtain the interaction potential between H and H⁻ fairly accurately at regions relevant to the production of H⁻. The accuracy of the position of the $^2\Sigma_u^+$ H₂⁻ curve lying below the threshold of dissociative attachment is, however, not clear.

Recently accurate measurements of the vibrational excitation cross section for H₂ via the formation of the

³⁶ W. Kolos and L. Wolnicwicz, J. Chem. Phys. **43**, 2429 (1965).

³⁷ G. J. Schulz, Phys. Rev. **113**, 816 (1959).

³⁸ J. C. Y. Chen and J. L. Peacher (to be published); *Proceedings of the Fifth International Conference on the Physics of Electronic and Atomic Collisions* (Publishing House Nauka, Leningrad, USSR, 1967), p. 335.

${}^2\Sigma_u^+ \text{H}_2^-$ state have been carried out by Ehrhardt *et al.* [H. Ehrhardt, H. Langhans, F. Linder, and H. S. Taylor, Abstract of the Twentieth Gaseous Electronics Conference San Francisco, 1967 (unpublished), p. 64; see also Ref. 37]. It was found that the cross section for the excitation of the first vibrational level of H_2 becomes appreciable right at the first vibrational excitation threshold (~ 0.5 eV). Examining the relevant portion of the ${}^2\Sigma_u^+ \text{H}_2^-$ curve (i.e., that portion lying below the dissociative attachment threshold) we found that this potential curve predicts moderately well the observed behavior for vibrational excitation. Since the ${}^2\Sigma_u^+ \text{H}_2^-$ state lies about 3.3 eV above the ${}^1\Sigma_g^+ \text{H}_2$ state (Fig. 8)

and has a half width $\frac{1}{2}\Gamma$ of about 1.3 eV (Fig. 7), one would expect, based on the Breit-Wigner resonance formula, that resonance effects due to the ${}^2\Sigma_u^+ \text{H}_2^-$ state should become appreciable at an energy *below* 2.0 eV (i.e., 3.3–1.3 eV).

The small discrepancy can be removed simply by modifying slightly the parameters in Eq. (3.12a) [see J. C. Y. Chen, in *Advances in Radiation Chemistry* (John Wiley and Sons, Inc., New York, 1968), Vol. I]. Detailed calculation of the resonant vibrational-excitation cross section with explicit consideration of the angular dependence of the scattered electrons is being carried out.

Lifetime of a Negative Helium Ion

D. J. NICHOLAS, C. W. TROWBRIDGE, AND W. D. ALLEN

Rutherford High Energy Laboratory, Chilton, Didcot, Berkshire, England

(Received 13 July 1967)

The lifetime of a negative ion of helium produced from He^+ by charge exchange in helium gas is measured and found to be 18.2 ± 2.7 μsec . This is consistent with the lower limit of 10 μsec previously determined. Total loss cross-section measurements in the energy range 20–70 keV are reported and compared with a previous published value at 17.5 keV. An investigation is also made of the destruction of the negative ions by thermal photons; this is found to be negligible at the temperatures involved, enabling an upper limit of 2.0×10^{-15} cm^2 to be set on the photodetachment cross section of He^- .

1. INTRODUCTION

SINCE Hiby¹ first proposed the existence of the negative ion of helium, a considerable amount of experimental and theoretical work has been carried out on it. The experimental work has been mainly directed at producing more intense ion beams, which are admirably suited for certain experiments in nuclear structure, and to the investigation of new processes for producing helium negative ions (Donnally and Thoeming²). Theoretical estimates of the binding energy of the ion have been made by Ta-You Wu,³ by Holøien,⁴ and by Holøien and Midtal,⁵ the latter results being largely borne out by the experimental work of Riviere and Sweetman⁶ and of Smirnov and Chibisov.⁷ Holøien and Midtal find that the only stable electronic configuration is the $(1s2s2p)4P_{5/2}$ with a binding energy of 0.075 eV with respect to the $(1s2s)3S$ metastable level. The $4P_{5/2}$ state is radiatively metastable and not subject to auto-ionization (Holøien and Midtal⁵). For spon-

aneous transitions from this state, the only available final state, consistent with angular momentum and parity conservation, is then the $(1s^2kf)^2F$ state. In calculating the lifetime of the $4P_{5/2}$ state, the matrix element connecting the stationary state to the $2P_{5/2}$ continuum state, the Coulomb, and spin-orbit operators have vanishing matrix elements. However, transitions can still proceed by means of a spin-spin interaction between two of the electrons and calculations on this basis by Pietenpol⁸ yield a lifetime of 1.7 msec. More recent calculations by Laughlin and Stewart⁹ have shown that this value is too large and more refined calculations using more complex wave functions give lifetimes which lie close to 4×10^{-4} sec for uncorrelated wave functions. Introducing correlated wave functions into their calculations increases this value by one order of magnitude. However, it is of interest to determine experimentally the lifetime of the ion.

2. PRINCIPLE OF MEASUREMENT

An ion such as He^- decaying in flight with lifetime τ will, under idealized conditions of perfect vacuum, undergo loss of intensity such that the current after time t will be proportional to $e^{-t/\tau}$. With the known minimum life of 10^{-6} sec, an ion velocity of the order

¹ J. W. Hiby, *Ann. Physik* **34**, 473 (1939).

² B. L. Donnally and G. Thoeming, *Phys. Rev.* **159**, 87 (1967).

³ Ta-You Wu, *Phil. Mag.* **22**, 837 (1936).

⁴ E. Holøien, *Arch. Math. Nature* **51**, 81 (1951).

⁵ E. Holøien and J. Midtal, *Proc. Phys. Soc. (London)* **A68**, 815 (1955).

⁶ A. G. Riviere and D. R. Sweetman, *Phys. Rev. Letters* **5**, 560 (1960).

⁷ B. M. Smirnov and M. I. Chibisov, *Zh. Eksperim. i Teor. Fiz.* **49**, 841 (1966) [English transl.: *Soviet Phys.—JETP* **22**, 585 (1966)].

⁸ J. L. Pietenpol, *Phys. Rev. Letters* **7**, 64 (1961).

⁹ C. Laughlin and A. L. Stewart, *Proc. Phys. Soc. (London)* **A88**, 893 (1966).